

# Nature of chiral phase transition in QED<sub>3</sub> at zero density

Hong-tao Feng<sup>1,5\*</sup>, Jian-Feng Li<sup>2,5</sup>, Yuan-mei Shi<sup>3,4,5</sup>, and Hong-shi Zong<sup>4,5,6†</sup>

<sup>1</sup>*Department of Physics, Southeast University, Nanjing, 211189, China*

<sup>2</sup>*College of Mathematics and Physics, Nantong University, Nantong 226019, China*

<sup>3</sup>*Department of Physics, Nanjing Xiaozhuang College, Nanjing 211171, China*

<sup>4</sup>*Department of Physics, Nanjing University, Nanjing, 210093, China*

<sup>5</sup>*State Key Laboratory of Theoretical Physics, Institute of Theoretical Physics, CAS, Beijing 100190, Peoples Republic of China and*

<sup>6</sup>*Joint Center for Particle, Nuclear Physics and Cosmology, Nanjing 210093, China*

Based on the feature of chiral susceptibility and thermal susceptibility at finite temperature, the nature of chiral phase transition around the critical number of fermion flavors ( $N_c$ ) and the critical temperature ( $T_c$ ) at a fixed fermion flavors number in massless QED<sub>3</sub> are investigated. It is showed that, at finite temperature the system exhibits a second-order phase transition at  $N_c$  or  $T_c$  and each of the estimated critical exponents is less than 1, while it reveals a higher-order continuous phase transition around  $N_c$  at zero temperature.

Keywords: QED<sub>3</sub>, chiral phase transition, chiral susceptibility, thermal susceptibility.

PACS numbers: 11.10.Kk, 11.15.Ex, 11.15.Tk, 11.30.Rd

## I. INTRODUCTION

The study of chiral phase transition (CPT) in (2+1)-dimensional quantum electrodynamics (QED<sub>3</sub>) has been an active subject for 30 years since Appelquist *et al.* found that CPT occurs when the flavor of massless fermions reaches a critical number  $N_c$  [1]. They arrived at this conclusion by analytically and numerically solving the Dyson-Schwinger equation (DSE) for the fermion self-energy in the lowest order approximation where the involved one-loop boson polarization is obtained by the free form of the fermion propagator. To indicate the value of  $N_c$ , D. Nash adopted an improved scheme and gave a larger  $N_c$  [2]. Later, several groups investigated the dependence of chiral symmetry breaking on  $N$  and some groups doubted the existence of  $N_c$  [3, 4]. This question was answered by P. Maris *et al.*, who used the coupled DSEs for the photon and fermion propagator to investigate the influence of the full vacuum polarization and vertex function on the fermion propagator and they found that the critical number of fermion flavors for dynamical mass generation of massless QED<sub>3</sub> lies between 3 and 4 [5–7].

Nevertheless, what is the order of CPT around  $N_c$  might be an interesting question. To reveal that, the authors of [1] studied the light scalar degrees of freedom and the order parameter of CPT near  $N_c$  and found that the phase transition is not second-order and is also unlike conventional first-order transition [8]. In addition, the results from Cornwall-Jackiw-Tomboulis effective potential also gave the same conclusion [9]. Although the above reveals the characteristic CPT, it is interesting to

adopt an alternative method to reanalyze the nature of this phase transition and see whether it is consistent with those results.

At finite temperature, the value of  $N_c$  should also vary and chiral symmetry restores as the temperature increases at a fixed  $N(< N_c)$ . In this case, the fermion propagator at finite temperature  $T$  can be written as

$$S^{-1}(T, P) = i\vec{\gamma} \cdot \vec{P} A_{\parallel}(P^2) + i\varpi_n \gamma_3 A_3(P^2) + B(P^2), \quad (1)$$

where  $\varpi_n = (2n + 1)\pi T$  and  $A$ ,  $B$  are the fermion wave-renormalization factor and self-energy, respectively. Adopting the lowest-order approximation of DSE and using Eq. (1), Dorey investigated the CPT of QED<sub>3</sub> at finite temperature and showed that QED<sub>3</sub> with dynamical chiral symmetry breaking (DCSB) undergoes CPT into chiral symmetric phase when the temperature reaches a critical value  $T_c$  and the corresponding  $N_c$  decreases with the increasing temperature [10].

The above conclusion holds in massless QED<sub>3</sub>. Then, another natural question may be raised: how does one chart the phase diagram of thermal QED<sub>3</sub> around  $T_c$  and whether or not the nature of CPT around  $N_c$  at finite temperature is the same as that at zero temperature. At the involved temperature, since the external fields are screened by thermal excitations and the boson gains a nonzero mass, the feature of CPT at  $N_c$  might be changed. However, as far as we know, the nature of CPT at  $N_c$  in thermal QED<sub>3</sub> has not been reported in the existing literature. Therefore, it is very interesting to study this problem.

In recent years, some works in lattice QCD [11–13] showed that the peak of chiral susceptibility should be an essential characteristic of CPT. Later, based on techniques of continuum field theory, several groups [14–19] also reached the same conclusion. Thus, chiral susceptibility is competent for studying the feature of phase transition in this nonperturbative system. Meanwhile, the

\*Email: fenght@seu.edu.cn

†Email: zonghs@chenwang.nju.edu.cn

thermal susceptibility give other ideal parameter to investigate the characteristic of CPT at finite temperature[20]. In this paper, we shall adopt the chiral and thermal susceptibilities to study the nature of chiral phase transition of QED<sub>3</sub> at finite temperature.

## II. FORMALISM FOR CHIRAL SUSCEPTIBILITY

The Lagrangian of QED<sub>3</sub> involving  $N$  fermion flavors of  $4 \times 1$  spinor reads

$$\mathcal{L} = \sum_{j=0}^N \bar{\psi}_j (\not{\partial} + ie \not{A} - m) \psi_j + \frac{1}{4} F_{\sigma\nu}^2 + \frac{1}{2\xi} (\partial_\rho A_\rho)^2. \quad (2)$$

In the absence of the mass term  $m\bar{\psi}\psi$ , QED<sub>3</sub> has chiral symmetry. There are several equivalent choices of the order parameter for chiral symmetry breaking; here we use the fermion chiral condensate

$$\langle \bar{\psi}\psi \rangle_m = \int \frac{d^3p}{(2\pi)^3} \text{Tr}[S(m, p)], \quad (3)$$

where  $S$  is the dressed fermion propagator and  $Tr$  denotes trace operation over Dirac indices of the fermion propagator. Based on Lorentz structure analysis, the involved massive/massless fermion propagator can be written as

$$S^{-1}(m, p) = i\gamma \cdot p E(p^2) + F(p^2), \quad (4)$$

$$S^{-1}(p) \equiv S^{-1}(0, p) = i\gamma \cdot p A(p^2) + B(p^2). \quad (5)$$

In the high energy limit, the fermion propagator reduces to the free one, i.e.,  $S_0^{-1}(p) = i\gamma \cdot p$  in the chiral limit and  $S_0^{-1}(m, p) = i\gamma \cdot p + m$  beyond the chiral limit. From this it can be seen that, with a small fermion mass  $m$ , the integral in Eq. (3) is divergent. In this case we should employ a renormalization procedure to deal with this divergence. A natural approach is to subtract the condensate of the free fermion field from the above value. That is to say, we define the renormalized fermion chiral condensate by

$$\langle \bar{\psi}\psi \rangle \equiv \langle \bar{\psi}\psi \rangle_m - \langle \bar{\psi}\psi \rangle_{mf}, \quad (6)$$

where  $\langle \bar{\psi}\psi \rangle_{mf}$  is the condensate of the free fermion gas. Below, we shall determine the transition point via the maximum of chiral susceptibility  $\frac{\partial \langle \bar{\psi}\psi \rangle}{\partial m}$  (see, e.g., Refs. [11, 21]) which is defined as[14]

$$\chi^c = \left. \frac{\partial \langle \bar{\psi}\psi \rangle}{\partial m} \right|_{m \rightarrow 0}. \quad (7)$$

This equation indicates that the chiral susceptibility measures the response of the chiral condensate (the order parameter) to an infinitesimal change of the fermion mass responsible for explicit breaking of chiral symmetry. Note here that we evaluate the chiral susceptibility and fermion chiral condensate in the chiral limit.

From Eqs. (3)-(5), we immediately arrive at the chiral susceptibility of QED<sub>3</sub> in chiral limit

$$\chi^c = 4N \int \frac{d^3p}{(2\pi)^3} \left\{ \frac{p^2 A^2 D - 2p^2 ABC - B^2 D}{[p^2 A^2 + B^2]^2} - \frac{1}{p^2} \right\}, \quad (8)$$

where

$$C(p^2) = \left. \frac{\partial E(p^2)}{\partial m} \right|_{m \rightarrow 0}, \quad D(p^2) = \left. \frac{\partial F(p^2)}{\partial m} \right|_{m \rightarrow 0}. \quad (9)$$

## III. ZERO TEMPERATURE

The next task is to obtain the four functions  $A, B, C, D$ . These functions can be obtained by solving the DSE for the massive fermion propagator,

$$S^{-1}(m, p) = S_0^{-1}(m, p) + \int \frac{d^3k}{(2\pi)^3} \times [\gamma_\sigma S(m, k) \Gamma_\nu(m; p, k) D_{\sigma\nu}(m, q)], \quad (10)$$

where  $\Gamma_\nu(m; p, k)$  is the full fermion-photon vertex and  $q = p - k$ . The coupling constant  $\alpha = e^2$  has dimension one, and provides us with a mass scale. For simplicity, in this paper temperature, mass and momentum are all measured in unit of  $\alpha$ , namely, we choose a kind of natural units in which  $\alpha = 1$ . From Eq. (5) and Eq. (18), we obtain the equation satisfied by  $E(p^2)$  and  $F(p^2)$

$$E(p^2) = 1 - \frac{1}{4p^2} \int \frac{d^3k}{(2\pi)^3} \text{Tr}[i(\gamma p) \gamma_\sigma S(m, k) \times \Gamma_\nu(m; p, k) D_{\sigma\nu}(m, q)], \quad (11)$$

$$F(p^2) = \frac{1}{4} \int \frac{d^3k}{(2\pi)^3} \times \text{Tr}[\gamma_\sigma S(m, k) \Gamma_\nu(m; p, k) D_{\sigma\nu}(m, q)]. \quad (12)$$

Another involved function  $D_{\sigma\nu}(q)$  is the full gauge boson propagator which is given by [17]

$$D_{\sigma\nu}(m, q) = \frac{\delta_{\sigma\nu} - q_\sigma q_\nu / q^2}{q^2 [1 + \Pi(m, q^2)]} + \xi \frac{q_\sigma q_\nu}{q^4}, \quad (13)$$

where  $\xi$  is the gauge parameter and  $\Pi(q^2)$  is the vacuum polarization for the gauge boson which is satisfied by the polarization tensor for gauge boson and reads

$$\Pi_{\sigma\nu}(m, q^2) = - \int \frac{d^3k}{(2\pi)^3} \text{Tr}[S(m, k) \gamma_\sigma S(m, q+k) \Gamma_\nu(m, p, k)]. \quad (14)$$

Using the relation between the vacuum polarization  $\Pi(m, q^2)$  and  $\Pi_{\sigma\nu}(q^2)$ ,

$$\Pi_{\sigma\nu}(m, q^2) = (q^2 \delta_{\sigma\nu} - q_\sigma q_\nu) \Pi(m, q^2), \quad (15)$$

we can obtain an equation for  $\Pi(q^2)$  which has ultraviolet divergence. Fortunately, it is present only in the longitudinal part and is proportional to  $\delta_{\sigma\nu}$ . We can remove the divergence by the projection operator

$$\mathcal{P}_{\sigma\nu} = \delta_{\sigma\nu} - 3 \frac{q_\sigma q_\nu}{q^2}, \quad (16)$$

and obtain a finite vacuum polarization[18].

Finally, we choose to work in the Landau gauge, since the Landau gauge is the most convenient and commonly used one. Once the fermion-boson vertex is known, we immediately obtain truncated DSEs for the propagators of the fermion and the gauge boson and then the chiral susceptibility near  $N_c$  is obtained. Of course, just as mentioned in Ref. [22],  $N_c$  occurs only in homogeneous system, i.e., all the involved functions in this issue for the fermion and boson propagators should satisfy homogeneity degrees.

### A. Rainbow approximation

The simplest and most commonly used truncated scheme for the DSEs is the rainbow approximation,

$$\Gamma_\nu \rightarrow \gamma_\nu, \quad (17)$$

since it gives us rainbow diagrams in the fermion DSE and ladder diagrams in the Bethe-Salpeter equation for the fermion-antifermion bound state amplitude. In the framework of this approximation, the coupled equation for massive fermion propagator reduces to

$$S^{-1}(m, p) = S_0^{-1}(m, p) + \int \frac{d^3 k}{(2\pi)^3} \gamma_\sigma S(m, k) \gamma_\nu D_{\sigma\nu}(m, q). \quad (18)$$

From Eq. (5) and Eq. (18), we obtain the equation satisfied by  $E(p^2)$  and  $F(p^2)$

$$E(p^2) = 1 - \frac{1}{4p^2} \int \frac{d^3 k}{(2\pi)^3} Tr[i(\gamma p)\gamma_\sigma S(m, k)\gamma_\nu D_{\sigma\nu}(m, q)],$$

$$(19) \text{ with } H(k^2) = A^2(k^2)k^2 + B^2(k^2) \text{ and}$$

$$\begin{aligned} C_1 &\equiv [B^2(k^2)C(k^2) - A^2(k^2)C(k^2)k^2 - 2A(k^2)B(k^2)D(k^2)] [1 + \Pi(q^2)] - A(k^2)H(k^2)\Pi'(q^2), \\ D_1 &\equiv [A(k^2)D(k^2)k^2 - B^2(k^2)D(k^2) - 2A(k^2)B(k^2)C(k^2)k^2] [1 + \Pi(q^2)] - B(k^2)H(k^2)\Pi'(q^2), \\ \Pi'_1 &\equiv [A(p^2)C(k^2) + A(k^2)C(p^2)] H(k^2)H(p^2) - 2A(k^2)A(p^2) [A(k^2)C(k^2)k^2 + B(k^2)D(k^2)] H(p^2) \\ &\quad - 2A(k^2)A(p^2) [A(p^2)C(p^2)p^2 + B(p^2)D(p^2)] H(k^2), \end{aligned}$$

where  $A$ ,  $B$ ,  $\Pi$  are obtained by Eqs. (21-23) at  $m = 0$ . By application of iterative methods, we can obtain  $A$ ,  $B$ ,  $\Pi$  and the above functions for the scalar vertex.

### B. Improved scheme for DSE

To improve the truncated scheme for DSE, there are several attempts to determine the functional form for the full fermion-gauge-boson vertex [24-27], but none of them completely resolve the problem. However, the

$$F(p^2) = \frac{1}{4} \int \frac{d^3 k}{(2\pi)^3} Tr[\gamma_\sigma S(m, k)\gamma_\nu D_{\sigma\nu}(m, q)], \quad (20)$$

In order to obtain these two functions, we start from the propagators with massive fermion. From the above two equations and some tricks proposed in Ref. [23], we obtain the three coupled equations for  $E(p^2)$ ,  $F(p^2)$  and  $\Pi(m, q^2)$ ,

$$E(p^2) = 1 + \frac{2}{p^2} \int \frac{d^3 k}{(2\pi)^3} \frac{E(k^2)(pq)(kq)/(q^2)^2}{G(k^2)[1 + \Pi(m, q^2)]} \quad (21)$$

$$F(p^2) = m + 2 \int \frac{d^3 k}{(2\pi)^3} \frac{F(k^2)/q^2}{G(k^2)[1 + \Pi(m, q^2)]}, \quad (22)$$

$$\begin{aligned} \Pi(m, q^2) &= \frac{2N}{q^2} \int \frac{d^3 k}{(2\pi)^3} \frac{E(k^2)E(p^2)}{G(k^2)G(p^2)} \times \\ &\quad [2k^2 - 4(k \cdot q) - 6(k \cdot q)^2/q^2], \quad (23) \end{aligned}$$

with  $G(k^2) = E^2(k^2)k^2 + F^2(k^2)$ .

Adopting Eqs. (9) and (21-23) and setting  $\Pi'(q^2) = \frac{\partial \Pi(m, q^2)}{\partial m} \Big|_{m \rightarrow 0}$ , we get the coupled equations for  $C(p^2)$ ,  $D(p^2)$  and  $\Pi'(q^2)$ ,

$$C(p^2) = \frac{2}{p^2} \int \frac{d^3 k}{(2\pi)^3} \frac{(p \cdot q)(k \cdot q)C_1/(q^2)^2}{H^2(k^2) [1 + \Pi(q^2)]^2}, \quad (24)$$

$$D(p^2) = 1 + 2 \int \frac{d^3 k}{(2\pi)^3} \frac{D_1/q^2}{H^2(k^2) [1 + \Pi(q^2)]^2}, \quad (25)$$

$$\Pi'(q^2) = \frac{2N}{q^2} \int \frac{d^3 k}{(2\pi)^3} \frac{[2k^2 - 4(k \cdot q) - 6(k \cdot q)^2/q^2] \Pi'_1}{H^2(k^2)H^2(p^2)}, \quad (26)$$

Ward-Takahashi identity (WTI)

$$(p - k)_\nu \Gamma_\nu(m; p, k) = S^{-1}(m, p) - S^{-1}(m, k), \quad (27)$$

provides us an effectual tool to obtain a reasonable ansatz for the full vertex [24]. The portion of the dressed vertex which is free of kinematic singularities, i.e. BC vertex, can be written as,

$$\Gamma_\nu(m, p, k) = \frac{E(p^2) + E(k^2)}{2} \gamma_\nu + \frac{F(p^2) - F(k^2)}{p^2 - k^2} (p + k)_\nu$$

$$+(\not{p} + \not{k}) \frac{E(p^2) - E(k^2)}{2(p^2 - k^2)} (p + k)_\nu. \quad (28)$$

Since the numerical results obtained using the first part of the vertex coincide very well with earlier investigations [6, 16], we choose this one as a reasonable ansatz

$$\Gamma_\nu^{BC_1}(m; p, k) \doteq \frac{1}{2} [E(p^2) + E(k^2)] \gamma_\nu \quad (29)$$

to be used in our calculation. Following the procedure in rainbow approximation, we also obtain the three coupled equations for  $E(p^2)$ ,  $F(p^2)$  and  $\Pi(m, q^2)$  in the improved truncated scheme for DSEs,

$$E(p^2) = 1 + \int \frac{d^3k}{(2\pi)^3} \frac{E(k^2)[E(p^2) + E(k^2)](pq)(kq)/(q^2)^2}{p^2 G(k^2)[1 + \Pi(m, q^2)]}, \quad (30)$$

$$F(p^2) = m + \int \frac{d^3k}{(2\pi)^3} \frac{[E(p^2) + E(k^2)]F(k^2)/q^2}{G(k^2)[1 + \Pi(m, q^2)]}, \quad (31)$$

$$\Pi(m, q^2) = \frac{N}{q^2} \int \frac{d^3k}{(2\pi)^3} \frac{E(k^2)E(p^2)[E(p^2) + E(k^2)]}{G(k^2)G(p^2)} [2k^2 - 4(k \cdot q) - 6(k \cdot q)^2/q^2], \quad (32)$$

and the corresponding unknown functions for  $C(p^2)$ ,  $D(p^2)$ ,  $\Pi'(q^2)$  are,

$$\begin{aligned} C(p^2) &= \frac{1}{p^2} \int \frac{d^3k}{(2\pi)^3} \frac{(pq)(kq)/q^2}{[1 + \Pi(q^2)]^2} \left\{ \frac{[C_1 - C_2][1 + \Pi(q^2)]}{H^2(k^2)} - \frac{A(k^2)[A(p^2) + A(k^2)]\Pi'(q^2)}{H(k^2)} \right\}, \\ D(p^2) &= 1 + \int \frac{d^3k}{(2\pi)^3} \frac{1}{[1 + \Pi(q^2)]^2} \left\{ \frac{[D_1 - D_2][1 + \Pi(q^2)]}{H^2(k^2)} - \frac{B(k^2)[A(p^2) + A(k^2)]\Pi'(q^2)}{H(k^2)} \right\}, \\ \Pi'(q^2) &= \frac{N}{q^2} \int \frac{d^3k}{(2\pi)^3} \frac{\Pi'_1 \Pi'_2 - 2\Pi'_3 \Pi'_4}{H^2(k^2)H^2(p^2)} [2k^2 - 4(k \cdot q) - 6(k \cdot q)^2/q^2], \end{aligned}$$

with

$$\begin{aligned} C_1 &\equiv \{2A(k^2)C(k^2) + A(p^2)C(k^2) + A(k^2)C(p^2)\}H(k^2), \\ C_2 &\equiv 2A(k^2)[A(p^2) + A(k^2)][A(k^2)C(k^2)k^2 + B(k^2)D(k^2)], \\ D_1 &\equiv \{D(k^2)[A(k^2) + A(p^2)] + B(k^2)[C(k^2) + C(p^2)]\}H(k^2), \\ D_2 &\equiv 2B(k^2)[A(p^2) + A(k^2)][A(k^2)C(k^2)k^2 + B(k^2)D(k^2)], \\ \Pi'_1 &\equiv [A(k^2)C(p^2) + A(p^2)C(k^2)][A(k^2) + A(p^2)] + A(k^2)A(p^2)[C(k^2) + C(p^2)], \\ \Pi'_2 &\equiv H(k^2)H(p^2), \\ \Pi'_3 &\equiv A(k^2)A(p^2)[A(p^2) + A(k^2)], \\ \Pi'_4 &\equiv [A(k^2)C(k^2)k^2 + B(k^2)D(k^2)]H(p^2) + [A(p^2)C(p^2)p^2 + B(p^2)D(p^2)]H(k^2), \end{aligned}$$

where  $A$ ,  $B$ ,  $\Pi$  are obtained by Eqs. (30-32) in the chiral limit.

### C. Chiral susceptibility around $N_c$

By application of numerical methods,  $A$ ,  $B$ ,  $\Pi$  and the functions for the scalar vertex can be obtained. The typical behaviors for the six functions  $A(p^2)$ ,  $B(p^2)$ ,  $C(p^2)$ ,  $D(p^2)$  and  $\Pi(q^2)$ ,  $\Pi'(q^2)$  are shown in Fig. 1. From Fig. 1 it can be seen that, excepting that  $A(p^2)$  and  $D(p^2)$  approach 1, the other functions vanish in the large momentum limit and all the six functions are almost constant in the infrared region.

Substituting the above functions into Eq. (8), we immediately obtain the value of chiral susceptibility and fermion chiral condensate with a range of fermion flavors. The results are plotted in Fig. 2. From this figure, we see that, with  $N$  increasing, the chiral susceptibility shows an obvious peak in the rainbow approximation and  $BC_1$  vertex approximation, while  $\langle \bar{\psi}\psi \rangle$  diminishes and vanishes at a critical number of fermion flavors where CPT occurs. Since each ansatz keeps different symmetry of the system,  $N_c$  depends a little on the choice of the ansatz for the dressed vertex. In addition, we also see that the susceptibility around  $N_c$  is apparently different from that at high temperature and high density [17]. The peak shows a neither divergent nor discontinuous behavior which il-

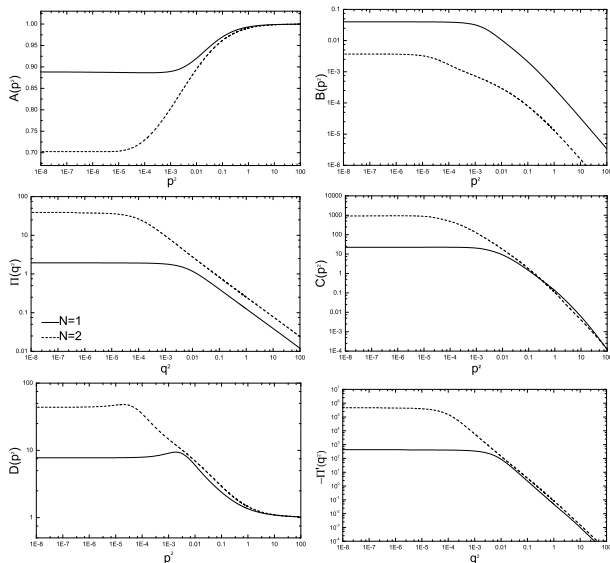


FIG. 1: The behavior of  $A(p^2)$ ,  $B(p^2)$ ,  $C(p^2)$ ,  $D(p^2)$ ,  $\Pi(q^2)$  and  $-\Pi'(q^2)$  in  $BC_1$  vertex approximation at  $N = 1, 2$ .

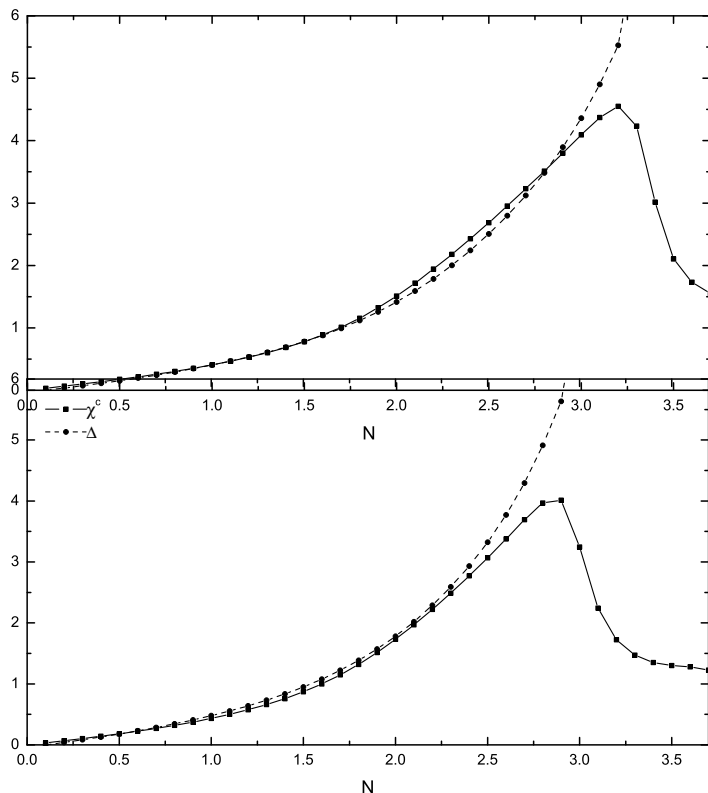


FIG. 2: The dependence of chiral susceptibility and fermion chiral condensate at zero temperature on  $N$  in the rainbow approximation (upper panel) and  $BC_1$  vertex approximation (lower panel), where  $\Delta = -\lg \frac{\langle \bar{\psi}\psi \rangle_N}{\langle \bar{\psi}\psi \rangle_{N=0}}$ .

illustrates that CPT at  $N_c$  is neither of first-order nor of second-order and thus is a higher-order continuous phase transition, which is consistent with the previous works [8, 9].

#### IV. FINITE TEMPERATURE

With the involved temperature,  $O(3)$  symmetry of the system reduce to  $O(2)$  and the gauge boson acquires a nonzero mass. The mass of the photon implies that external electric fields are screened by thermal excitations [10] and so we expect that the feature of CPT may be changed by the excitations.

##### A. Truncated DSE

To give an insight of CPT, we shall adopt DSE for the fermion propagator and techniques of temperature field theory to calculate the chiral and thermal susceptibility at finite temperature with the increasing  $N$  and analyze the transition of  $QED_3$  near  $N_{Tc}$ , and also reveal the nature of CPT at the critical temperature  $T_{Nc}$  with a fixed  $N$ .

Now, let us give a short review of some studies on the effect of the wave function renormalization factor  $A_{\parallel}$  and  $A_3$ . Just as mentioned in Sec. I, the chiral phase transition (CPT) in  $QED_3$  was first studied in Ref. [1], where it is found that CPT occurs at  $N_c \approx 3.24$ . They arrived at this conclusion by solving the lowest order DSE for the fermion self-energy. Later, some groups adopted improved schemes for DSE to study this problem and obtained qualitatively similar results with  $N_c \approx 3.3$  [5, 6]. This suggests that the lowest order DSE for the fermion propagator is a suitable approximation to study CPT at finite temperature.

At finite temperature, to obtain a qualitative picture of chiral susceptibility, we employ a familiar framework to obtain the scalar part of the inverse fermion propagator where the zero frequency approximation of boson polarization is widely adopted [10, 17, 28, 29]. In addition, the conclusions in Ref. [30] illustrated that, by summing over the frequency modes and taking suitable simplifications, the qualitative aspects of the result obtained under the zero frequency approximation for the wave function renormalization  $A$ ,  $E$  and the fermion mass function  $B$ ,  $F$  do not undergo significant changes. From this, we also ignore the frequency dependence of fermion self-energy  $B$  and then the corresponding DSE for the scalar part of inverse fermion propagator reads [17]

$$\begin{aligned}
 F(P^2) &= m + 2T \int \frac{d^2K}{(2\pi)^2} \sum_{n=-\infty}^{\infty} \frac{F(K^2)/[Q^2 + \Pi(Q)]}{\omega_n^2 + K^2 + F^2(K^2)} \\
 &= \int \frac{d^2K}{(2\pi)^2} \frac{F(K^2) \tanh \frac{\epsilon_k}{2T}}{\mathcal{E}_k [Q^2 + \Pi(Q)]}, \quad (33)
 \end{aligned}$$

where  $\mathcal{E}_k = \sqrt{K^2 + F^2(K^2)}$  and the zero frequency boson polarization

$$\Pi(Q) = \frac{NT}{\pi} \int_0^1 dx \left\{ \ln \left( 4 \cosh^2 \frac{M(x)}{2T} \right) - \frac{m^2 \tanh \frac{M(x)}{2T}}{TM(x)} \right\}, \quad (34)$$

with  $M^2(x) = m^2 + x(1-x)Q^2$ .

With the general equation for the chiral susceptibility (8), we can obtain the chiral susceptibility at finite temperature

$$\begin{aligned} \chi^c &= 4NT \sum_n \int \frac{d^2P}{(2\pi)^2} \\ &\times \left\{ \frac{[\varpi_n^2 + P^2 - B^2(P^2)]D(P^2)}{[\varpi_n^2 + P^2 + B^2(P^2)]^2} - \frac{1}{\varpi_n^2 + P^2} \right\} \\ &= 2N \int \frac{d^2P}{(2\pi)^2} \times \\ &\left\{ \frac{D(P^2)}{\mathcal{E}_p} \left[ \frac{P^2}{\mathcal{E}_p^2} \tanh \frac{\mathcal{E}_p}{2T} + \frac{B^2(P^2) \text{sech}^2 \frac{\mathcal{E}_p}{2T}}{2T\mathcal{E}_p} \right] \right. \\ &\left. - \frac{1}{\mathcal{E}_{p0}} \left[ \frac{P^2}{\mathcal{E}_{p0}^2} \tanh \frac{\mathcal{E}_{p0}}{2T} \right] \right\}, \quad (35) \end{aligned}$$

where  $\mathcal{E}_{p0} = \sqrt{P^2}$ . The unknown function in the above equation,  $D(P^2)$ , is obtained by  $F(P^2)$

$$\begin{aligned} D(P^2) &= \lim_{m \rightarrow 0} \frac{\partial F(P^2)}{\partial m} = 1 + \int \frac{d^2K}{(2\pi)^2} \frac{1}{\mathcal{E}_k [Q^2 + \Pi(Q)]} \times \\ &\left\{ \left[ \frac{D(K^2)K^2}{\mathcal{E}_k^2} - \frac{B(K^2)\Pi'(Q)}{Q^2 + \Pi(Q)} \right] \tanh \frac{\mathcal{E}_k}{2T} \right. \\ &\left. + \frac{D(K^2)B^2(K^2)}{2T\mathcal{E}_k} \text{sech}^2 \frac{\mathcal{E}_k}{2T} \right\}, \quad (36) \end{aligned}$$

with  $\Pi'(Q) = \lim_{m \rightarrow 0} \frac{\partial \Pi(Q)}{\partial m}$ . From Eq. (34), we easily find that  $\Pi'(Q) = 0$ .

Similarly, thermal susceptibility measures the response of the chiral condensate to an infinitesimal change of temperature

$$\begin{aligned} \chi^T &= \frac{\partial \langle \bar{\psi} \psi \rangle}{\partial T} \\ &= \int \frac{d^2P}{(2\pi)^2} \mathcal{E}_p \left[ B'(P^2) \tanh \frac{\mathcal{E}_p}{2T} - \frac{B^2(P)B'(P) \tanh \frac{\mathcal{E}_p}{2T}}{\mathcal{E}_p^2} \right. \\ &\left. + B(P^2) \text{sech}^2 \frac{\mathcal{E}_p}{2T} \left( \frac{B'(P^2)B(P^2)}{2T\mathcal{E}_p} - \frac{\mathcal{E}_p}{2T^2} \right) \right] \quad (37) \end{aligned}$$

with  $B' = \frac{\partial B}{\partial T}$ .

## B. Numerical results

After solving the above coupled DSEs by means of the iteration method, we can now calculate chiral fermion

condensate and the above two susceptibilities, which can be regarded as a function of  $N$  given by Eq. (35) and (37) with a range of temperature. The typical behaviors of the susceptibilities and condensate are shown in Fig. 3 and Fig. 4. The upper lines of Fig. 3 give the behavior

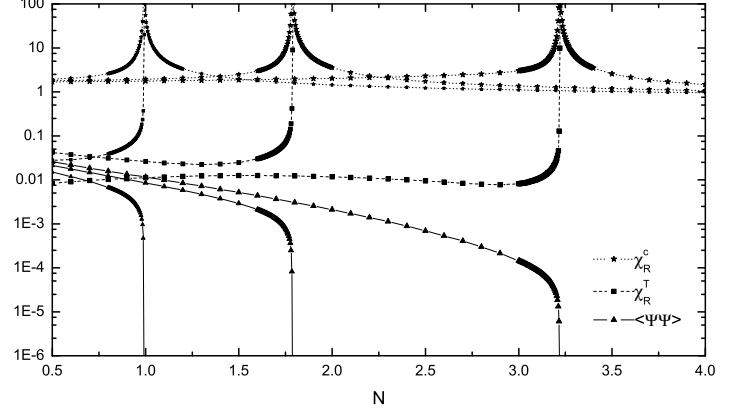


FIG. 3: The behaviors of chiral susceptibility and thermal susceptibility around the critical fermion flavors with several  $T$  (where  $\chi_R^c = \frac{\chi^c}{N}$ ,  $\chi_R^T = -\chi^T$ , from left to right denote  $T = 2.5 \times 10^{-2}, 10^{-2}, 10^{-3}$ ).

of chiral susceptibility and the lower lines in this figure show the fermion chiral condensate, while the other lines between the two group denote that of thermal susceptibility. As is shown in Fig. 3, for any given temperature,  $\chi^c$  almost keeps a constant for small and large  $N$ , while it shows an apparent peak at some critical number of fermion flavors. This number depends on the temperature and diminishes as the temperature increases. When  $N$  reaches a critical value  $N_{Tc}$ , the appearance of vanishing fermion chiral condensate and divergence peak of  $\chi^T$  occur at the same point. This critical fermion flavors also decreases with the increase of  $T$ , which is similar to the results in the previous works [10, 28, 29]. By all appearances, at any temperature the peak of each susceptibility lies at  $N_{Tc}$ . Moreover, near  $N_c$ , the chiral susceptibility at finite temperature shows a different behavior from that at zero temperature. From Fig. 3, we also see that the chiral and thermal susceptibilities exhibits a very narrow, pronounced and in fact divergent peak at  $N_{Tc}$ , which is a typical characteristic of second-order phase transition driven by the restoration of chiral symmetry at finite temperature.

For a fixed  $N$ , with the increasing temperature, chiral symmetry restores at a temperature  $T_{Nc}$  and each susceptibility exhibits the same behavior around the critical point. From Fig. 4, we see that the chiral and thermal susceptibility reveal their infinite value at  $T_{Nc}$  which also illustrate the typical second-order phase transition.

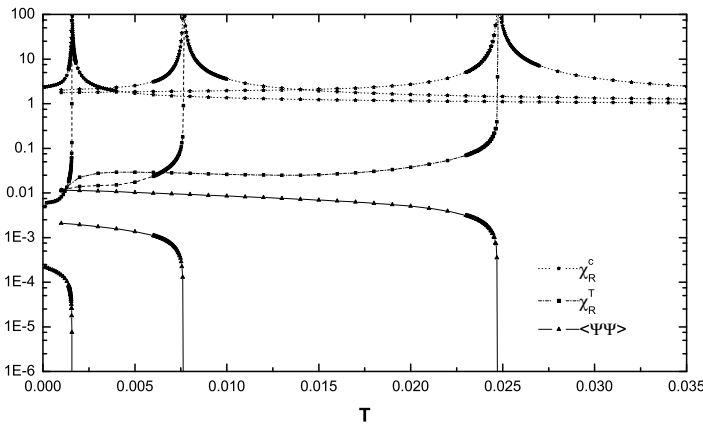


FIG. 4: The behaviors of chiral and thermal susceptibilities around the critical temperature with several  $N$  (from left to right denote  $N = 3, 2, 1$ ).

### C. Critical exponents

Just as shown above, the chiral phase transition at finite temperature is second order, a natural question is: what are the critical exponents? Now, let us try to answer this question. Around the critical points, the phase transitions are characterized by the corresponding critical exponents which are an important contemporary goal to exhibit the feature of CPT. We find that the fermion chiral condensate near the critical point reveals

$$\begin{aligned} \langle \bar{\psi}\psi \rangle &\sim t^\alpha, \quad N = \text{const}, \\ \langle \bar{\psi}\psi \rangle &\sim n^\beta, \quad T = \text{const}, \end{aligned} \quad (38)$$

with the reduced temperature  $t = 1 - T/T_c$  and the reduced fermion flavors number  $n = 1 - N/N_c$ . The typical behavior of the condensate near the point of CPT can be seen in Fig. 5 and find that, in each figure, the slope of the line of infrared fermion self-energy  $B(0)$  is same to that of  $\langle \bar{\psi}\psi \rangle$  which indicates that  $B(0)$  and  $\langle \bar{\psi}\psi \rangle$  illustrate the same value of critical exponent in massless QED<sub>3</sub>.

Numerically, for a fixed  $N$ , the estimated  $\alpha$  at  $t \rightarrow 0^+$  and also the estimated  $\beta$  at  $n \rightarrow 0^+$  with several  $T$  are given as

N	$\alpha$	T	$\beta$
1	0.507	$10^{-3}$	0.487
2	0.538	$10^{-2}$	0.401
3	0.416	0.025	0.423

In addition, near the point of phase transition, each of the two susceptibilities at  $t, n \rightarrow 0^+$  reveals its critical feature as

$$\begin{aligned} \chi^c &\sim t^{-\gamma^c}, \quad N = \text{const}, \\ \chi^T &\sim t^{-\gamma^T}, \quad N = \text{const}, \\ \chi^c &\sim n^{-\delta^c}, \quad T = \text{const}, \\ \chi^T &\sim n^{-\delta^T}, \quad T = \text{const}, \end{aligned}$$

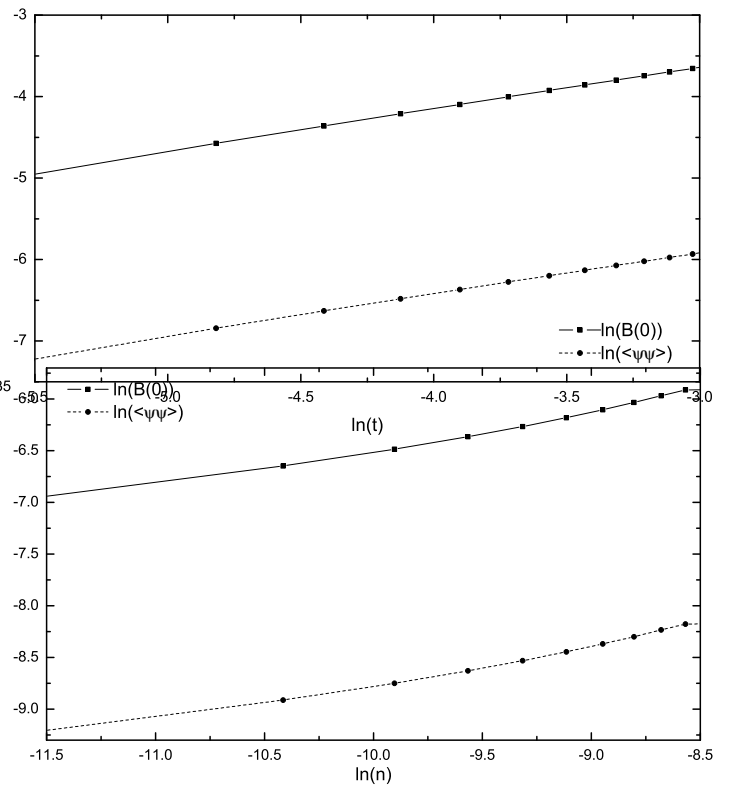


FIG. 5: The critical behavior of  $\langle \bar{\psi}\psi \rangle$  and  $B(0)$  near the point of CPT with a range of  $t$  at  $N = 1$  (top) and a range of  $n$  at  $T = 0.025$  (bottom).

and their critical behaviors can be found in Fig. 6.

From the numerical results, we estimate the critical exponents of the susceptibility with several  $N$  or  $T$  and give  $\gamma$ ,  $\delta$  in the following table:

N	$\gamma^c$	$\gamma^T$	T	$\delta^c$	$\delta^T$
1	0.679	0.350	$10^{-3}$	0.769	0.622
2	0.769	0.354	$10^{-2}$	0.813	0.712
3	0.476	0.274	0.025	0.931	0.455

It is shown that each of the critical exponents is less than 1 and, in the same boundary condition, the critical exponent of  $\chi^c$  is larger than that of  $\chi^T$ .

## V. CONCLUSIONS

The primary goal of this paper is to investigate the nature of chiral phase transition of QED<sub>3</sub> near the critical value, including critical number of fermion flavors and critical temperature through a continuum study of the chiral and thermal susceptibilities. Based on the suitable approximation of truncated DSEs for the fermion propagator and numerical model calculations, we study the behavior of the two susceptibilities near the critical point of CPT in QED<sub>3</sub>. It is found that, with the rise of the number of fermion flavors, the appearance of the

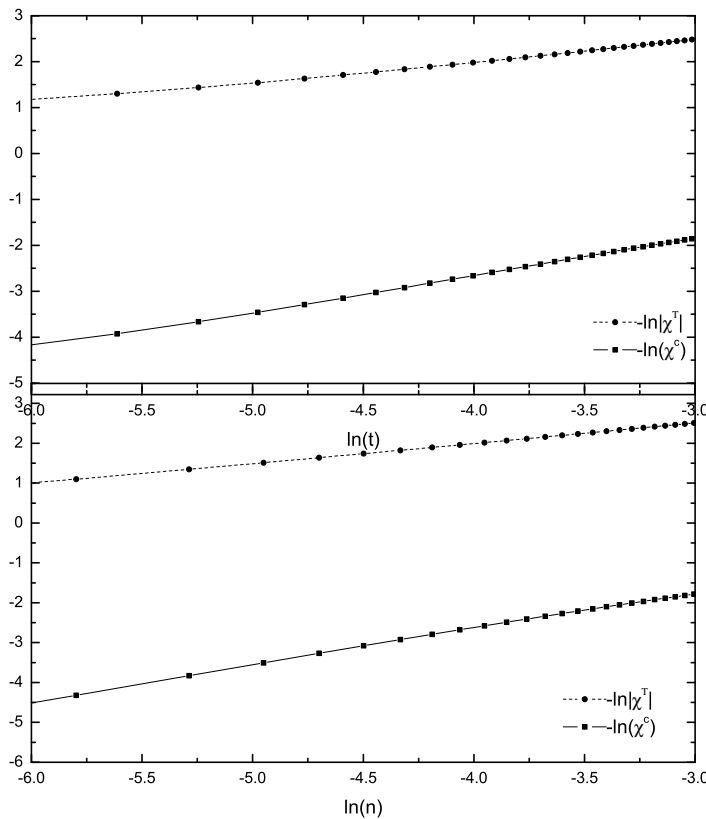


FIG. 6: The critical behavior of two susceptibilities near the point of CPT with a range of  $t$  at  $N = 1$  (top) and a range of  $n$  at  $T = 0.025$  (bottom).

peak of chiral susceptibility and CPT occur at the same critical point, but the peak reveals apparently different behavior at zero and finite temperature.

At zero temperature the chiral susceptibility near the critical number of fermion flavors reveals a finite and continuous peak, which exhibits that CPT is neither of first order nor of second order, and thus it should be a continuous phase transition of higher order. However, apart from zero temperature, each of chiral and thermal susceptibility at either critical fermion flavors or chiral temperature shows a large and in face divergent peak which illustrates a typical characteristic of second-order phase transition driven by chiral symmetry restoration in thermal QED<sub>3</sub>.

Finally, though the analysis for the critical exponents, it is found that the critical exponents of chiral/thermal susceptibility which characterize the chiral phase transition is between 0.2 and 1 and, in the same boundary condition, the critical exponent of thermal susceptibility is less than that of chiral susceptibility.

## VI. ACKNOWLEDGEMENTS

This work was supported in part by the National Natural Science Foundation of China (under Grant Nos. 11105029, 11275097, and 11347212) and the Research Fund for the Doctoral Program of Higher Education (under Grant No 2012009111002) and by the Fundamental Research Funds for the Central Universities (under Grant No 2242014R30011).

- 
- [1] T. Appelquist, D. Nash, and L.C.R. Wijewardhana, Phys. Rev. Lett. **60**, 2575 (1988).
  - [2] D. Nash, Phys. Rev. Lett. **62**, 3024 (1989).
  - [3] D.C. Curtis, M.R. Pennington and D. Walsh, Phys. Lett. B **295**, 313 (1992).
  - [4] M.R. Pennington and D. Walsh, Phys. Lett. B **253**, 246 (1991).
  - [5] P. Maris, Phys. Rev. D **54**, 4049 (1996).
  - [6] C.S. Fischer, R. Alkofer, T. Dahm, and P. Maris, Phys. Rev. D **70**, 073007 (2004).
  - [7] A. Bashir, C. Calcano-Roldan, L.X. Gutierrez-Guerrero, and M.E. Tejeda-Yeomans, Phys. Rev. D **83**, 033003 (2011).
  - [8] T. Appelquist, J. Terning, and L.C.R. Wijewardhana, Phys. Rev. Lett. **75**, 2081 (1995).
  - [9] H.T. Feng, B. Wang, W.M. Sun, and H.S. Zong, Phys. Rev. D **86**, 105042 (2012).
  - [10] N. Dorey and N.E. Mavromatos, Phys. Lett. B **266**, 163 (1991).
  - [11] F. Karsch and E. Laermann, Phys. Rev. D **50**, 6954 (1994).
  - [12] M. Cheng et al., Phys. Rev. D **75**, 034506 (2007).
  - [13] L. K. Wu, X. Q. Luo, and H. S. Chen, Phys. Rev. D **76**, 034505 (2007).
  - [14] M. He, Y. Jiang, W. M. Sun, and H. S. Zong, Phys. Rev. D **77**, 076008 (2008).
  - [15] L. Chang, Y. X. Liu, C. D. Roberts, Y. M. Shi, W. M. Sun, and H. S. Zong, Phys. Rev. C **79**, 035209 (2009).
  - [16] M. He, F. Hu, W. M. Sun, and H. S. Zong, Phys. Lett. B **675**, 32 (2009).
  - [17] H.T. Feng, S. Shi, P.L. Yin, and H.S. Zong, Phys. Rev. D **86**, 065002 (2012).
  - [18] H.T. Feng, B. Wang, W.M. Sun, and H.S. Zong, Eur. Phys. J. C **73**, 2444(2013).
  - [19] Y. Zhao, L. Chang, W. Yuan, and Y.X. Liu, Eur. Phys. J. C **56**, 483 (2008).
  - [20] A. Höll, P. Maris, and C.D. Roberts, Phys. Rev. C **59**, 1751 (1999).
  - [21] C.S. Fisher, J. Luecker, and J.A. Muller, Phys. Lett. B **702**, 438 (2011).
  - [22] A. Bashir, A. Raya, I.C. Cloet, and C.D. Roberts, Phys. Rev. C **78**, 055201 (2008).
  - [23] H.T. Feng, W.M. Sun, F. Hu, and H.S. Zong, Inter. J. Mod. Phys. **A20**, 2753 (2005).
  - [24] J. S. Ball and T. W. Chiu, Phys. Rev. D **22** 2542 (1980).
  - [25] D.C. Curtis and M.R. Pennington, Phys. Rev. D **42**, 4165 (1990).
  - [26] A. Ayala and A. Bashir, Phys. Rev. D **64**, 025015 (2001).
  - [27] A. Bashir and A. Raya, Phys. Rev. D **64**, 105001 (2001).
  - [28] N. Dorey and N.E. Mavromatos, Nucl. Phys. **B386**, 614 (1992).
  - [29] I.J.R. Aitchison and M. Klein-Kreisler, Phys. Rev. D **50**,

1068 (1994).

[30] A. Ayala and A. Bashir, Phys. Rev. D **67**, (2003) 076005.